

FIRST RESULTS FROM MULTIFREQUENCY INTERFEROMETRY. A COMPARISON OF DIFFERENT DECORRELATION TIME CONSTANTS AT L, C AND X BAND

Alessandro Parizzi¹, Xiao Ying Cong², and Michael Eineder¹

¹DLR, Remote Sensing Technology Institute, Muenchener Strasse 20, 82234 Wessling, Germany

²TU Munchen, Arcis Strasse 21, 80333 Muenchen, Germany

ABSTRACT

The measurement of displacement from SAR images, using either interferometric or correlation techniques, is always carried out from a comparison between two or more acquisitions separated in time. It is therefore necessary to evaluate the level of phase decorrelation between the two acquisitions in order to understand the quality of the measures that can be obtained. The change of radar resolution cells in time is known to be the main responsible of the gradual decorrelation of the interferometric phase. However, a model that physically describes this process, is at the moment not available. Exploiting the test sites from GITEWS and Exupery, German projects focussed on determination of geo-risks, an analysis of the decorrelation time constants was performed on SAR data from PALSAR, ASAR and TerraSAR-X. Time series of the coherence have been computed and compared with simple statistical models. The time constants were analyzed as a measure of temporal decorrelation, in order to forecast the precision of displacement measures also for future missions. The extracted parameters were finally compared with the type of land covering using optical data and land use maps in order to determine a qualitative relationship between them and extend their validity in a more global context.

Key words: DInSAR, Decorrelation.

1. INTRODUCTION

Several studies on the nature of decorrelation in SAR interferograms have been carried out and models have been defined, in particular, for the effects of the acquisitions geometries on interferometric coherence [1] [2]. It is difficult to understand how the complex correlation decreases with the temporal separation between two images. We must first assume that within the same pixel, the contributions of the distributed elements somehow change, reducing the correlation to previous acquisitions. This change has to be interpreted as the physical change in the resolution cell and is therefore a completely different phenomena with respect to geometric decorrelation

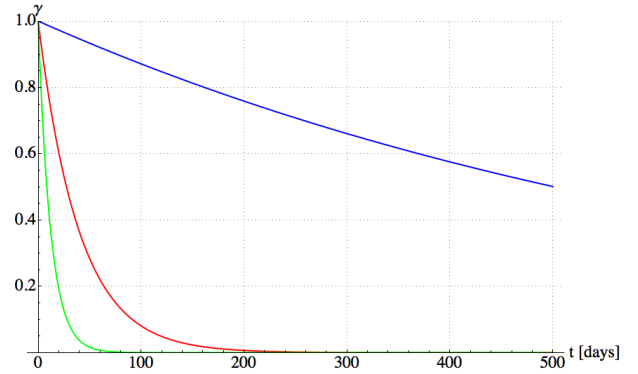


Figure 1. Decorrelations functions for L, C and X band (blue, red and green respectively) according to Eq. 1 .

that can be deterministically modelled and even compensated for by spectral shift filtering [2]. .

2. TEMPORAL DECORRELATION MODELS AND THEORY

Let us start by considering the model that links the loss of coherence with a slow displacement of the distributed targets inside the resolution cell [1] .The assumption in this model is that the cell is composed of a certain number of points with the same response which are randomly distributed in space. The source of the decorrelation is modelled as a drift movement that changes their mutual positions. This generates an exponential decrease as follows:

$$\gamma(t) = e^{-\frac{1}{2} \left(\frac{4\pi}{\lambda}\right)^2 \sigma^2 \Delta t} \quad (1)$$

where σ is the standard deviation of target movement per time unit and λ is the wavelength. Starting from these assumptions, we can plot the function in Eq. 1 over time for different wavelengths, Fig. 1. The model can be generalized to the exponential model [3], Eq. 2

$$\gamma(t) = \gamma_0 e^{-\frac{t}{\tau(\lambda)}} \quad (2)$$

where γ_0 is the instantaneous decorrelation due to the thermal noise and τ is the time constant which depends

on λ . Within a time τ , the correlation will drop to $1/e$, i.e. to 0.36. According to the model previously described [1] (Eq. 2) the decorrelation rate should be proportional to $\propto \frac{1}{\lambda^2}$ that for the case L-band / C-Band should be almost 18 times larger, Fig. 1. Observing the coherence images estimated from a stack of SAR acquisition it is immediately evident the exponential trend of the correlation in time. However, in some areas, the values estimated for long temporal baseline saturate to a certain level. These behaviours can be hardly explained using a simple time constant. Recently, an alternative definition of temporal decorrelation based on Markov statistics have been introduced in literature . In this case we suppose that the scatterers present within the pixel can have two different states, coherent or not coherent [3]. Therefore the definition of correlation becomes:

$$\gamma(t) = \frac{E[n_{un}(t)]}{n_{tot}} \quad (3)$$

Where n_{un} is the number of scatterers that did not change their response and n_{tot} is the total number of reflectors in the resolution cell. Considering a changing rate of τ the general expression can be derived as :

$$dE[n_{un}(t)] = -\frac{E[n_{un}(t)]}{\tau} \quad (4)$$

$$E[n_{un}(t)] = n_{tot}e^{-\frac{t}{\tau}} \quad (5)$$

Moreover, considering more than one group of points, the Eq. 5 can be written as the sum of contributions from different τ_i . The weights p_i are the probabilities of each group defined as the number of reflectors with this time constant divided by the total number of points:

$$\gamma(t) = \sum_i p_i e^{-\frac{t}{\tau_i}} \quad (6)$$

For modelling our case we will simply need to consider three different classes:

- the points that at the beginning of our observation time window are already decorrelated with $\tau = 0$;
- the points that will decorrelate with time constant τ ;
- the points that will not decorrelate in our observation time window with $\tau = \infty$;

From Eq. 6 we can finally write our model as:

$$\gamma(t) = (\gamma_0 - \gamma_k)e^{-\frac{t}{\tau}} + \gamma_k \quad (7)$$

where τ is the time constant and γ_0 and γ_k are respectively the start and end coherence. Eq. 7 will be used in this paper to characterize the decorrelation process. The three parameters will be estimated and compared for different wavelengths and finally with the land cover.

Table 1. Main acquisitions parameters for the sensors involved in the experiments.

Sensor	λ	θ_{inc}	ρ_{ground}	T_{rev}	Pol.
PALSAR	0.239	38	4x17 - 4x9	46	HH
ERS	0.056	23	4x20	35	VV
TerraSAR-X	0.031	19	3x3	11	VV

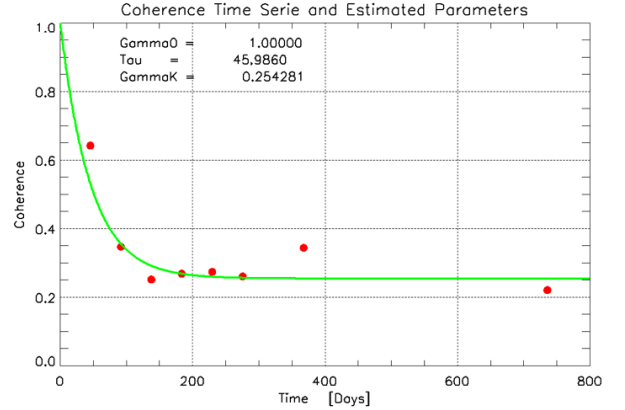


Figure 2. Example of Coherence Time Series fitting. Estimated parameters are printed in the upper left part of the figure, green line is the fitted trend and red dots are the coherence measures.

3. METHODOLOGY

In order to measure the decorrelation behaviours some experiments have been carried out. First of all it was necessary to generate three data stacks at the different wavelengths. Data from ALOS PALSAR (FBS and FBD), ERS 1-2 and TerraSAR-X Stripmap have been used in this framework with parameters shown in Table 1 . Every dataset has been processed using DLR GENESIS Software coregistering the acquisitions of every stack to a previously selected master scene. Then, in order to limit the spectral shift effects [2] , only the small-baseline interferograms have been computed. The maximum spectral shift was set to 15% of the bandwidth which, in the case of the acquisition geometries in Table 1 , translate into maximum normal baselines of about 2 Km, 300 m and 800 m for L, C and X bands respectively. The coherence maps were generated using at least 100 Looks. According to [4] averaging over this amount of independent pixels will permit to reduce the bias in coherence estimation to less than 0.07. Moreover, in order to decrease the noise of the estimation, an average is computed between the maps having the same temporal separation. The fitting of the model (Eq. 7) is finally computed for each pixel across the stack of coherence images.

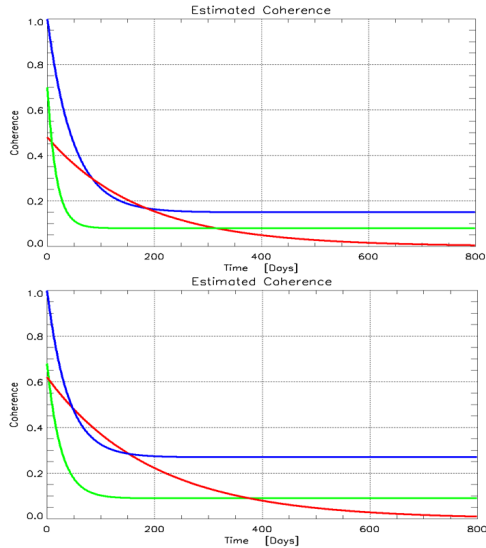


Figure 3. Decorrelations Functions retrieved from the real data. Examples from two areas in the test site, see Fig.4. L, C and X band (blue, red and green respectively)

4. RESULTS AND DISCUSSION

In this section the results obtained from the real data will be analyzed and two comparisons will be performed:

- Comparison of the estimated parameters at the different wavelengths;
- Comparison of the estimated parameters with land cover (L-band);

4.1. Multi-Frequency Comparison

To compare the decorrelation properties of the different wavelengths the island of Kos in the Aegean sea has been selected as test site. In this area a sufficient number of data from the three sensors were available and the effects of geometric decorrelation can be considered not so critical because of the type of landscape (morphology and land cover). The model of Eq. 7 was fitted and finally some common areas have been chosen for the comparison. The median of each parameter was extracted and the decorrelation functions have been plotted together in order to better show their different behaviour in time. The Figure 3 shows a comparison of the estimated coherence functions in time for two different areas of the test site. Even if we observe clearly that the global behaviour of correlation is somehow proportional to the wavelength, it is difficult to extract an empirical formula to describe the relation between parameters and wavelength. The different scatter properties of the ground are probably responsible of the different trends but this would require a full scatter modelling of the resolution cell. Moreover the de-

pendence of the estimated parameters from the resolution and the polarization is still to be investigated.

4.2. Comparison with Land Cover

The relation between the estimated parameters and land cover is clear if we compare a map of the estimates with ground truth. For this analysis the L-Band was considered. The behaviour of γ_k was in fact particularly interesting in evaluating the long term correlation capabilities of this band. The maps have therefore been geocoded and then overlapped with an optical image for a qualitative analysis and then with a land classification map [5] that has permitted quantitative comparison. The overlay in Fig. 4 and the histograms in Fig. 6 show how the residual coherence is distributed according to the type of land cover. However, the difference in ground resolution between the GlobCover and our maps is significant. Therefore, in order to have a sufficient number of points on which to base the analysis, only the three main types of land use have been analyzed in detail. The three classes are, Rainfed Croplands that includes mainly agricultural fields, Mosaic Croplands that represent a quite large range of land cover types (small vegetation, shrublands [5]) and finally sparse (< 15%) vegetated land cover. This class shows a saturated coherence in time of 0.2 averagely that in some cases can reach more than 0.4. Areas characterized by agriculture, present mainly close to the coast, are of course more affected by a very fast decorrelation, that saturate to a much smaller value. Significant values of γ_k can also be found where there is small vegetation and shrublands as shown in Fig. 6 .

5. CONCLUSIONS

- Temporal Decorrelation is a complex process but its net effect can be described with a relatively small set of parameters
- This set of parameters is highly correlated with the land cover.
- The dependence of decorrelation on the wavelength seems to be more complicated than expected and is probably related to the scattering properties.
- For the evaluation of long term coherence capabilities not only the decorrelation time constants τ must be considered but also the residual correlation γ_k

ACKNOWLEDGMENTS

PALSAR and ERS images were provided by ESA under AO.3520. The research work is funded by the German Federal Ministry of Education and Research in the framework of the GITEWS and Exupery projects.



Figure 4. Overlay between the γ_k map estimated for L-band data and Google Earth. Red rectangles are the areas mentioned in Fig. 3

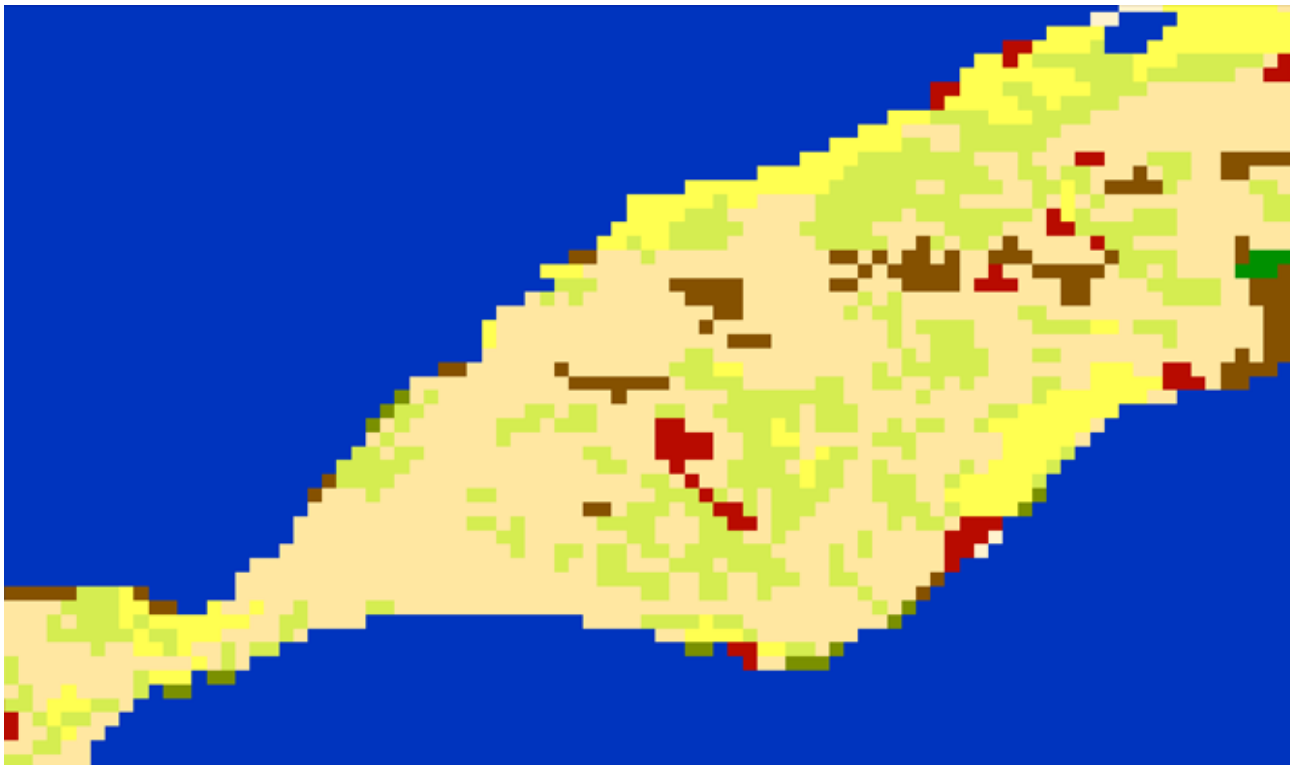


Figure 5. Land Cover Map from GlobCover database [5].

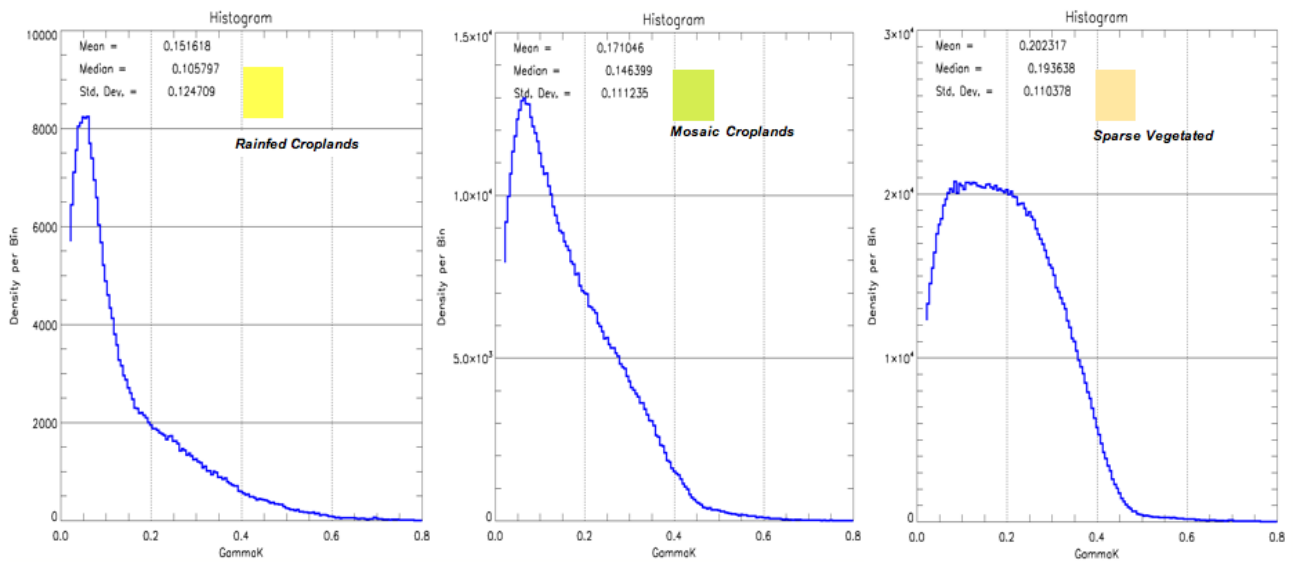


Figure 6. Statistics of γ_k according to the land cover.

REFERENCES

- [1] H.A. Zebker and J. Villasenior, *Decorrelation in interferometric radar echoes* IEEE Trans. Geosci. Remote Sens. Vol 30, No. 5 Sept. 1992
- [2] F. Gatelli et al., *The wavenumber shift in SAR interferometry* IEEE Trans. Geosci. Remote Sens. Vol 32, No. 4, Jul. 1994
- [3] F. Rocca *Modeling Interferogram Stacks* IEEE Trans. Geosci. Remote Sens. Vol 45, No. 10, Oct. 2007
- [4] R. Touzi, A. Lopes, P.W. Vachon *Coherence Estimation for SAR Imagery* IEEE Trans. Geosci. Remote Sens. Vol 37 No. 1 January 1999
- [5] Ionia GlobCover web page <http://ionial.esrin.esa.int/>